Structural Engineering and Mechanics, *Vol. 57, No. 6 (2016) 1125-1142*
DOI: http://dx.doi.org/10.12989/sem.2016.57.6.1125

Efficiency assessment of L-profiles and pipe fore-poling pre-support systems in difficult geological conditions: a case study

Ayub Elyasi[*1], Taher Moradi[2a], Javad Moharrami[2b], Saeid Parnian[2c], Akbar Mousazadeh[3d] and Sepideh Nasseh[4e]

[1]*Department of Mining Engineering, Tarbiat Modares University, Tehran, Iran*
[2]*Consultant Engineering Institute of Iman Sazan, Tehran, Iran*
[3]*Department of Civil Engineering, Islamic Azad University of Naghadeh, Naghadeh, Iran*
[4]*Department of Geology, Ferdowsi University of Mashhad, Mashhad, Iran*

(Received September 25, 2015, Revised January 24, 2016, Accepted February 11, 2016)

Abstract. Tunneling is one of the challenging tasks in civil engineering because it involves a variety of decision making and engineering judgment based on knowledge and experience. One of the challenges is to construct tunnels in risky areas under shallow overburden. In order to prevent the collapse of ceilings and walls of a large tunnels, in such conditions, either a sequential excavation method (SEM) or ground reinforcing method, or a combination of both, can be utilized. This research deals with the numerical modeling of L-profiles and pipe fore-poling pre-support systems in the adit tunnel in northwestern Iran. The first part of the adit tunnel has been drilled in alluvial material with very weak geotechnical parameters. Despite applying an SEM in constructing this tunnel, analyzing the results of numerical modeling done using FLAC3D, as well as observations during drilling, indicate the tunnel instability. To improve operational safety and to prevent collapse, pre-support systems, including pipe fore-poling and L-profiles were designed and implemented. The results of the numerical modeling coupled with monitoring during operation, as well as the results of instrumentation, indicate the efficacy of both these methods in tunnel collapse prevention. Moreover, the results of modeling using FLAC3D and SECTION BUILDER suggest a double angle with equal legs (2L100×100×10 mm) in both box profile and tee array as an alternative section to pipe fore-poling system while neither L80×80×8 mm nor 2L80×80×8 mm can sustain the axial and shear stresses exerted on pipe fore-poling system.

Keywords: sequential excavation method; alluvial material; numerical modeling; L-profiles; pipe fore-poling; monitoring

1. Introduction

∗Corresponding author, Ph.D. Student, E-mail: a.elyasi1986@yahoo.com
[a]M.Sc. Graduated, E-mail: moradi.taher@gmail.com
[b]M.Sc. Graduated, E-mail: j.moharrami85@yahoo.com
[c]M.Sc. Graduated, E-mail: saeid.parnian@gmail.com
[d]M.Sc. Graduated, E-mail: mousazadeh.ak613@yahoo.com
[e]Ph.D. Student, E-mail: sepideh_nasseh@yahoo.com

http://www.techno-press.org/?journal=sem&subpage=8 ISSN: 1225-4568 (Print), 1598-6217 (Online)

Tunneling in difficult geological conditions represents a thrust to the development of innovative techniques, or to the improvement of existing ones, devised to allow for an efficient tunnel excavation whereby ensuring the stability. Many equipment and technical provisions have been first introduced to face difficult conditions met in particular tunnel projects and have been later adopted in other similar situations, often after specific improvements (Mair 2008, Singh and Goel 2006).

A soft ground medium often causes difficulties in tunneling, due to its poor mechanical properties and great water bearing capacity. The stress release induced by the excavation causes weakening and possible localized failure at the face and at the roof. In the case of shallow tunneling, this effect can grow quickly and lead to large surface subsidence or even collapse.

In some cases, the tunnel face is partitioned to have temporary drifts in order to promote face stability and to reduce surface deformations and settlements; this method is referred to as the sequential excavation method (SEM) (FHWA 2009).

Another suitable method is applying special reinforcement techniques such as the umbrella arch method (UAM) that is commonly used to ensure tunnel stability (Ocak 2008). This method has been widely studied (Carrieri *et al*. 1991, 2002, Lunardi 2000, Yoo and Shin 2003, Kim *et al*. 2005). Furthermore, many field cases of excavated tunnels that used the UAM have been reported (Barisone *et al*. 1982, Gangale *et al*. 1992, Murata *et al*. 1996, Shin *et al*. 1999, Haruyama *et al*. 2001, Sekimoto *et al*. 2001, Kamata and Mashimo 2003, Shin *et al*. 2008, Aksoy and Onargan 2010, Elyasi *et al*. 2015).

As underground excavation designs become larger and more complex, numerical analyses are required to investigate difficult ground conditions. In such conditions, reinforcement or strengthening as a pre-support system is required prior to excavation. The UAM is turning to a popular method due to its time and cost efficiency in comparison with other pre-support methods such as ground freezing, jet grouted columns and pipe jacking (Volkmann and Schubert 2007).

Umbrella Arch Method (UAM) is commonly used for tunnel design in order to reinforce the ground around the tunnel and stabilize tunnel face. It consists of installing longitudinal bars or metal tubes at the periphery of the tunnel face, usually on the third or the quarter upper part of the circumference, resting on the last lining. This system is designed to limit decompressions and protect the excavation section from all surfaces of potential rupture (Fethi 2015).

Designing pipe-reinforced headings require determination of various factors such as length, stiffness, cross section (thickness and diameter) of pipes, installation angle, distances between pipes, overlapping length and grouting pressure. The distances between pipes are governed by grouting pressure. Consequently, in many cases the determination of pipe length is the main concern in the design of pipe reinforcement with grouting (Shin *et al*. 2008).

In design practice, the length of a pipe is defined at the tunnel crown. However, appropriate pipe length at the spring line also needs to be evaluated. In practice, however, generally the pipe length at the spring line is the same as that of the crown (Shin *et al*. 2008). The most common variations of the umbrella arc dimensions are presented in Table 1.

Table 1 Common variation of the umbrella arc dimensions (Shin *et al*. 2008)

Characteristics	Pipe size	Pipe length	Overlapping	Pipe distance	Water/cement ratio	Pipe inclination
Amount	OD 114 mm t=6 mm	12-30 m	1-4 m	0.33-0.8 m	0.5-2	<15 degree

Table 2 Geotechnical properties of material obtained from the borehole

Depth up	Depth to	Soil type	γ_d (g/cm^3)	γ_w (g/cm^3)	E (kg/cm^2)	Direct shear C (kg/cm^2)	Direct shear $\Phi°$
0	3	CL	2.03	2.08	76.8		
3	6	SC	1.96	2.03		0.11	27
6	9	SC-SM					
9	12	CL	2.07	2.24		0.15	27
12	15	CL	2.05	2.10		0.15	29
15	18	CL	1.98	2.03	35.67		
18	21	SC-SM		2.08			
21	24	SC-SM	2.00	2.08		0.09	31
24	27	CL		2.08			
27	30	SC-SM		2.08			

Table 3 Geotechnical properties of undisturbed samples

Sample No.	γ_d (g/cm3)	Direct Shear C (kg/cm^2)	Direct Shear $\Phi°$	Soil Type	LL	PI
1	1.75	0.07	29	SC-SM	24	5
2	1.65	0.08	27	SC	30	10
3	1.53	0.09	27	SC	32	14
4	1.72	0.07	28	SM		NP
5	1.7	0.08	27	SC	29	11

In this research, modeling and designing of two pre-support systems, pipe fore-poling and L-profiles (spiling), have been addressed in order to be implemented as the pre-support system of the adit tunnel in northwestern Iran. In the end, the performance of these two systems has been evaluated based on observations and instrumentation data.

2. Geology of study area

The great tunnel of Zagros is located in northwest of Iran. An adit tunnel will be constructed to access the main tunnel. This adit tunnel has been designed to be 1.354 km long and have a downward slope of 10.25%.

In the study area, a borehole 30 m deep was drilled to obtain the required geotechnical data. Results of the lab experiments on the samples extracted from the borehole are given in Table 2, where γ_d is the dry density, γ_w is the wet density, E is the elastic modulus, C is the cohesion and Φ is the friction angle of the medium.

To verify the input parameters in the stability analysis, undisturbed samples were selected from the working face and tunnel walls. Different experiments were then conducted on these samples and the results are presented in Table 3, where γ_d is the dry density, C is the cohesion, $\Phi°$ is the friction angle, LL is the liquid limit and PI is the plastic index of the medium.

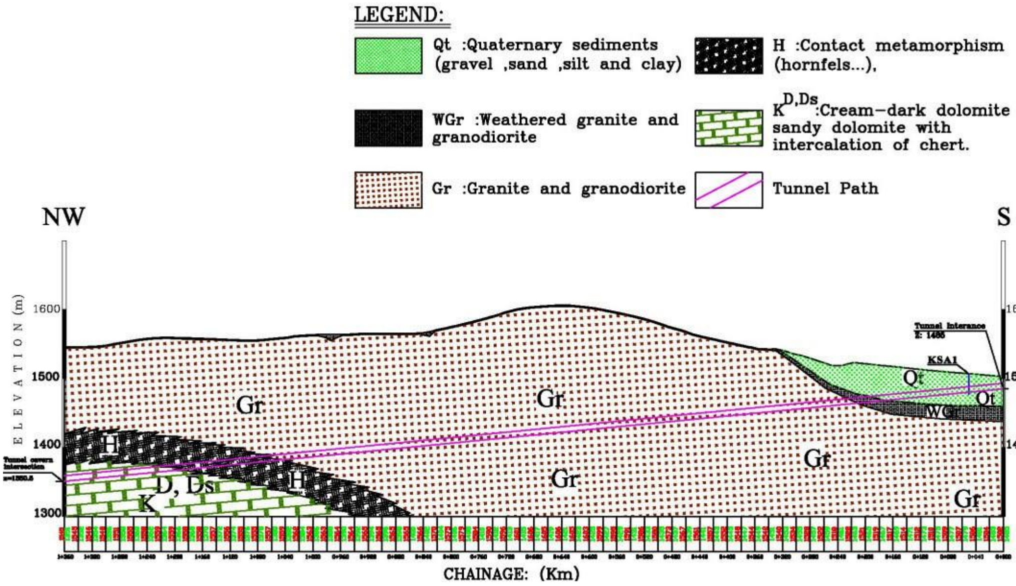

Fig. 1 Geological cross-section along the adit tunnel

Table 4 Component of initial support system

Support component	Number
Steel support	Lattice girder by 0.5 m spacing
Systematic Bolt	2 @32, L=3.0 m
Wire mesh	φ6@10 mm*10 mm
Shotcrete thickness (cm)	30
Excavation round (m)	0.5

Fig. 1 illustrates the geological cross-section along the adit tunnel. The most significant features of the material in this section are incoherence and very low plasticity index. Regarding the above facts and the material properties, it is clear that the materials are highly sensitive to disturbance, which can result in their collapse in different parts of the tunnel.

3. Excavation and installation of pre-support system

Regarding the studies conducted and the weakness of the geotechnical parameters of the alluvial materials in the beginning part of the adit tunnel route and in order to maintain the appropriate safety level during operation, the first part is to be drilled using the SEM. Therefore, first of all, the top section of the tunnel is drilled and the primary support system implemented. Characteristics of the support system are presented in Table 4. The top section includes a semi-circle with a radius of 4.05 m and a rectangular area as large as 60 cm under the semi-circular area. When this section is drilled about 15-30 m, the drilling of the lower section (bench) will start. After installing the bench support system, invert concreting as high as 60 cm will start. Also, to neutralize the bending moments and shear forces on the system, two rows of nailing (one after

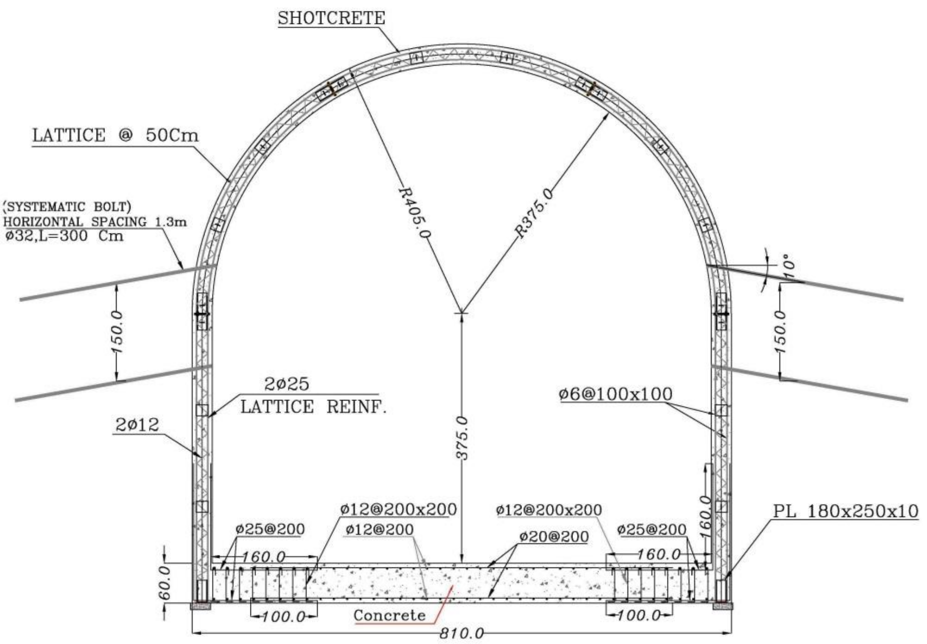

Fig. 2 Adit tunnel cross-section in the alluvial part

 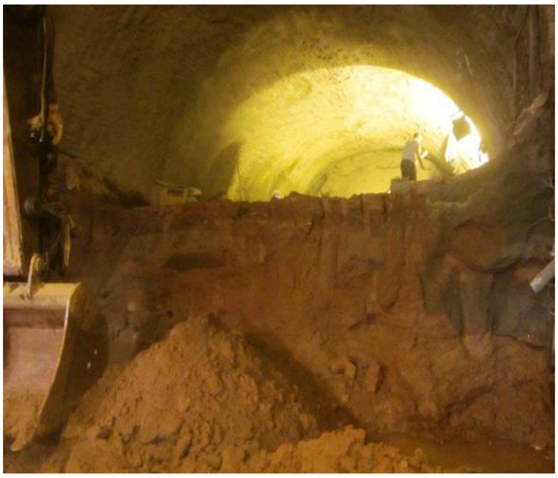

Fig. 3 Top and bench excavation and installation of the support system

installing a lattice ceiling girder, and the other after installing a lattice girder on the bench wall) in 1.3 m parts and 1.5 m away from each other were installed. The cross-section of the tunnel is shown in Fig. 2 and some images of the top and bench sections of the tunnel are shown in Fig. 3.

3.1 Numerical modeling

In this research, FLAC3D was used in order to study the stability analysis. The failure criterion assumed in these analyses was the Mohr-Coulomb criterion. To solve the model, after the geometry of the model was created, the following conditions were defined for the program: initial conditions, material properties along the tunnel route (SC, SM, etc.; according to Table 2 and 3), boundary conditions and fixing the model boundaries. Then the model was run until it reached the primary balance. The far-field stresses are applied on the models boundary as initial condition. Where σ_V is the vertical in-situ stress. σ_H and σ_h are the maximum and minimum horizontal stresses, respectively. Note that the initial and boundary condition for the model are as follows. The stresses are used to establish initial equilibrium conditions within the model. Also the lateral boundaries are fixed in the *XY* direction, the lower boundaries are fixed in the *XYZ* direction.

The next phase in modeling would be drilling the top section of the tunnel with a 0.5-m step, and implementing the support system and solving the model after each step of the drilling up to the 20-m point. Characteristics of the support system, including the buried triangular lattice girder, shotcrete and nailing, are shown in Tables 5, 6 and 7 respectively.

Finally, the following steps were taken: simultaneous drilling of the top and bench sections of the tunnel with steps as long as 0.5 m, implementing the support system, and running the model after each step of the drilling (in each phase of running the model, the distance between the top and the bench sections is constant and equal to 20 m (See Fig. 4).

Table 5 Lattice girder properties

E (GPa)	σ_c (MPa)	σ_t (MPa)	**ν**	spacing (m)
200	240	240	0.3	0.5

Table 6 Shotcrete properties

E (GPa)	**γ** (kg/m3)	σ_c (MPa)	**ν**
20	2200	21	0.15

Table 7 Nailing properties

E (GPa)	Diameter (mm)	Length (m)	Tensile Strength (KN)
200	32	3	0.16

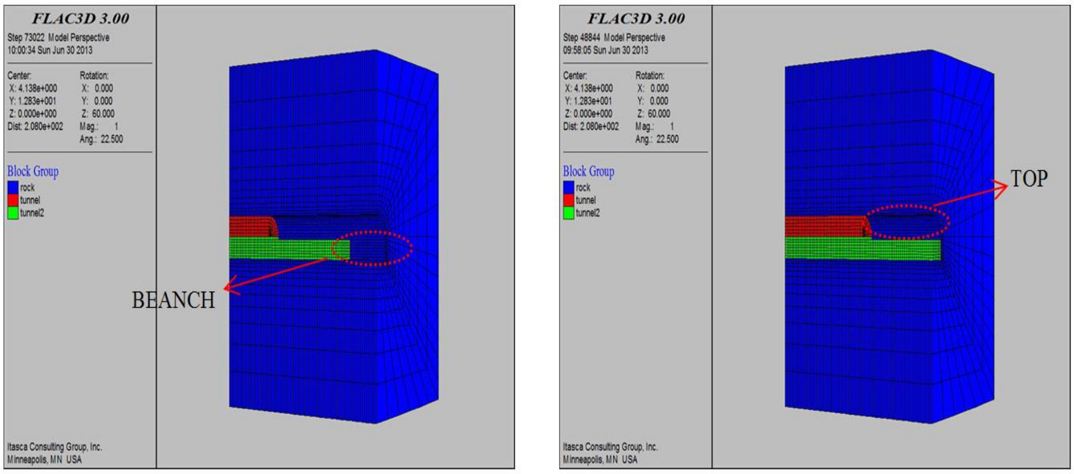

Fig. 4 Sequential excavation method (top and bench) in modeling with FLAC3D

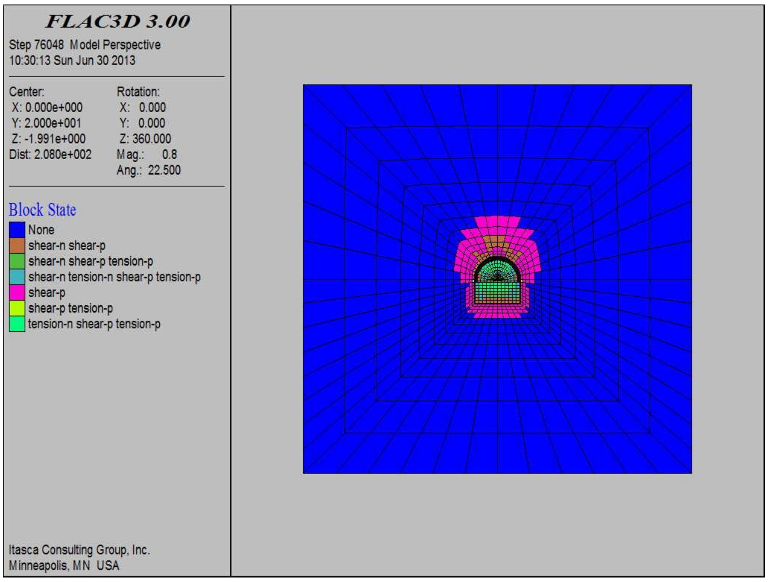

Fig. 5 Plastic zone around the tunnel without the pre-support system

Fig. 6 Tunnel instability (without the pre-support system)

3.2 Stability analysis without the pre-support system

A plan of the plastic zone formed around the tunnel is shown in Fig. 5. As can be seen, the vastness of the plastic zone around the tunnel leads to an increased dead load on the tunnel support system. This could lead to instability in the working face of the tunnel, in regards to the geological conditions of the site.

In practice, drilling in the aforementioned conditions led to some collapses in the walls and the ceiling of the tunnel (Fig. 6). This justifies use of the UAM pre-support system as one of the practical methods in drilling this tunnel.

Table 8 Umbrella arch properties

Characteristics	Pipe diameter (mm)	Pipe thickness (mm)	Pipe length (m)	Overlapping (m)	Row No.	Pipe distance (m)	Rows spacing (m)
Amount	90	9	9	2.5	2	0.5	0.25

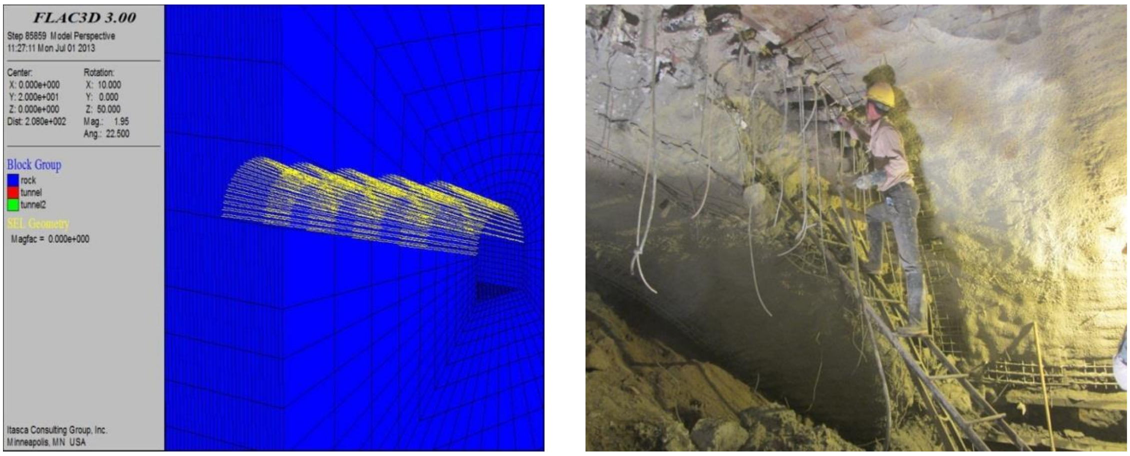

Fig. 7 Umbrella arch model (left) and its implementation (right)

Table 9 Maximum amounts of force, moment, and stress on the pipes during the top and bench excavation

N_x (MN)	N_y (MN)	N_z (MN)	M_y (MN-m)	M_z (MN-m)	σ_x (MPa)	σ_y (MPa)	σ_z (MPa)
0.418	0.525	0.155	0.325	0.267	3.34	42.05	78.04

3.3 Impact of the umbrella arch installation on the tunnel stability

Since the UAM imposes high expenses on a project on one hand, and requires a relatively long time to implement on the other, decisions about the method need to be made according to the requirements of the project. Therefore, the necessity of the umbrella arch was examined using numerical modeling as well as studying the conditions of the tunnel construction without applying this system. Regarding the afore-mentioned facts, a pre-support umbrella arch system with the properties shown in Table 8 was designed.

The process of modeling is similar to the phases mentioned in “numerical modeling” except that, in the latter case, an umbrella arch system with the features shown in Table 9 is installed prior to any drilling.

The plastic zone around the tunnel with an installed umbrella arch pre-support system is shown in Fig. 8. As can be seen, because of the pipe fore-poling, there has been a significant decrease in the plastic zone around the tunnel and, therefore, the tunnel will be more stable. Moreover, comparison between the displacements indicates that displacement in the crown and tunnel face decreased 30-40 percent.

Results show that deformations and the force on the pipes will differ based on the progression of drilling steps. The maximum force (which is vertical) usually occurs near the tunnel face. The maximum deformation occurs from 0.5-0.75 of the pipe length. The location of the maximum

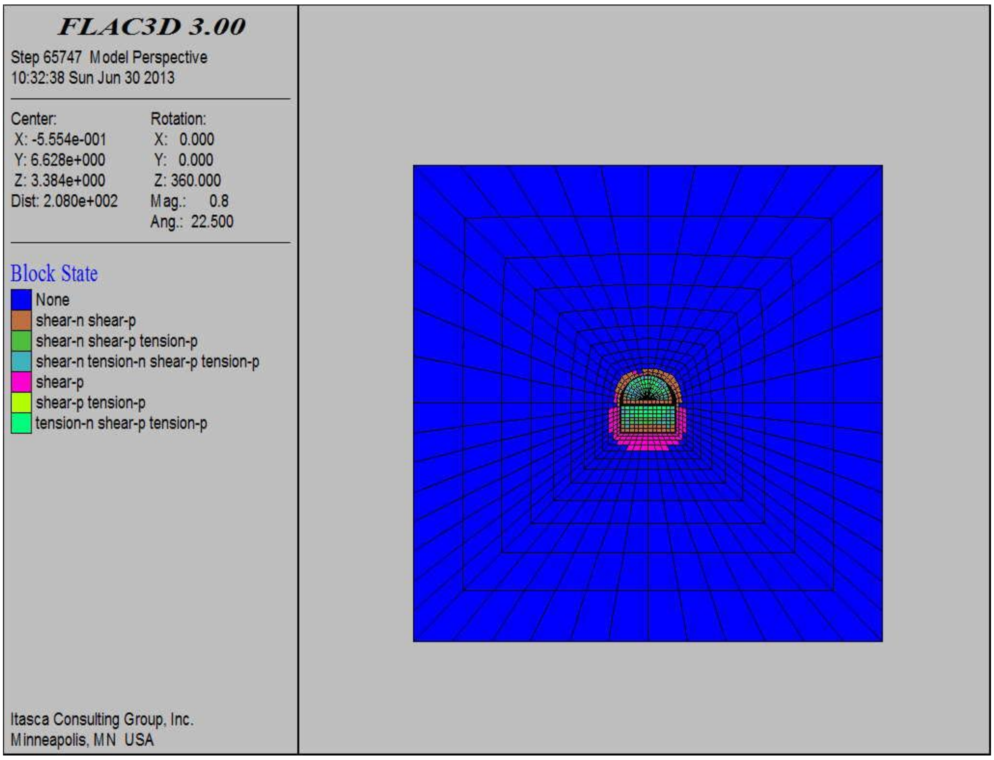

Fig. 8 Plastic zone around the tunnel with the pre-support system

force along the vertical axis is 1 m ahead of the tunnel face. The moment distribution related to this force also follows the same trend.

To study the possibility of yield and failure in the umbrella arch, first of all, its strength is calculated using a combination of pipe and concrete with a weight average. Regarding the 28-day strength of the grout with a water-cement ratio of 0.5 (α=0.5) and a 240 MPa yield strength of the steel, the strength of the umbrella arch is equal to 170 MPa.

The maximum amounts of force, moment and stress on the pipes during the top and bench excavation are listed in Table 9.

In Table 9, σ_y and σ_z are from the bending, and σ_x is from the axial force. Although these values did not occur simultaneously in one section, for comparison, all stress values were added up, being equal to 123.4 MPa. It can be seen that the aggregate stress value is less than the pipes' strength. Therefore, the pipes will not reach the yield point value and will not fail.

4. Replacement of pipe fore-poling system with double equal angles (L-profiles)

Although the discussed pipe fore-poling system was executed along more than 50 m of the adit tunnel successfully, some executive problems were involved. So application of L-profiles instead of pipe fore-poling system was suggested. In this regard, the pipe fore-poling system was substituted by 2L100×100×10 mm and also 2L80×80×8 mm using Section Builder software.

Table 10 Grouting parameters in uniaxial compression test

Compressive Strength (MPa)	Young's Modulus (MPa)	Compressive Strength (MPa)	Young's Modulus (MPa)	
Twenty eight-day		Seven-day		grout
11.42	2569	8.26	911	*w/c*=0.5

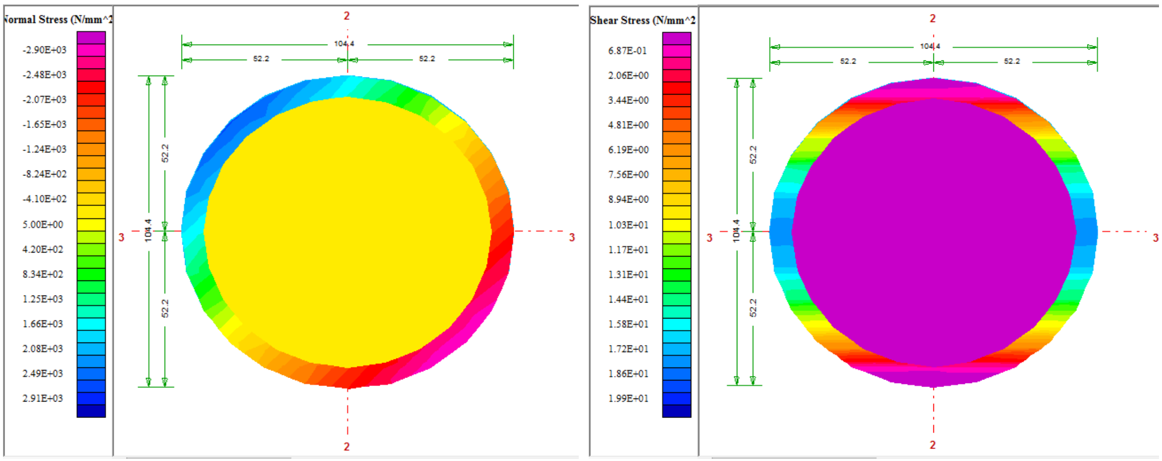

Fig. 9 Distribution of axial (left) and shear (right) stresses in pipe fore-poling system

4.1 Stress distribution in pipe fore-poling system

During the installation of pipe fore-poling system, the proportion of water to cement (w/c) for grout filling the annular gap equals 0.5. Strength parameters of the grout is presented in Table 10. In pipe fore-poling design, the seven-day parameter of grouting has been used.

Fig. 9 demonstrates the normal and shear stresses contours for pipe fore-poling system under axial load and specific bending moment. The pipe fore-poling system consists of steel pipes and jet grouted columns.

Based on Fig. 9, the range of axial stress is between 2900 to 2910 N/mm^2 while the range of shear stress is between 0.687 to 19.9 N/mm^2.

Moreover, it can be recognized that the values of normal and shear stresses are lower in injected grout compared with the steel pipes.

4.2 Substitution of pipe fore-poling system with L-profiles

In Tables 11 and 12, a summary of geometric properties as well as axial and shear stresses distributions of the sections (pipe fore-poling system, 2L100×100×10 mm, 2L80×80×8 mm and single sections) are presented.

According to Tables 11 and 12, the equivalent section for pipe fore-poling system is 2L100×100 ×10 mm (both box profile and tee array) so that they are able to meet the requirements of area and moment of inertia.

These two equivalent sections have higher areas and moments of inertia rather than pipe fore-poling section. Based on the investigations, none of the single-section L-profiles (L100×100×10

Table 11 Properties of pipe fore-poling and double equal angle sections

Moment of Inertia (Main Axis) (mm^4)	Area (mm^2)	Section Type
2.61×10^6	2198.6	Pipe fore-poling
0.737×10^6	1216	L80×80×8 mm
1.80×10^6	1900	L100×100×10 mm
1.47×10^6	2432	2L80×80×8 mm (tee array)
3.60×10^6	3800	2L100×100×10 mm (tee array)
2.18×10^6	3432.4	2L80×80×8 mm (box profile)
4.44×10^6	31600	2L100×100×10 mm (box profile)

Table 12 Stress distribution in pipe fore-poling system and L-profiles

Shear stress (N/mm^2)		Axial stress (N/mm^2)		Section type
Max	Min	Max	Min	
19.9	0.687	2910	-2900	Pipe fore-poling
46.9	1.62	11100	-11100	L80×80×8 mm
30	1.04	5710	-5700	L100×100×10 mm
21.9	0.754	4320	-4410	2L80×80×8 mm (tee array)
13.7	0.472	2210	-2260	2L100×100×10 mm (tee array)
21.6	0.746	3620	-3570	2L80×80×8 mm (box profile)
13.7	0.471	1860	-1840	2L100×100×10 mm (box profile)

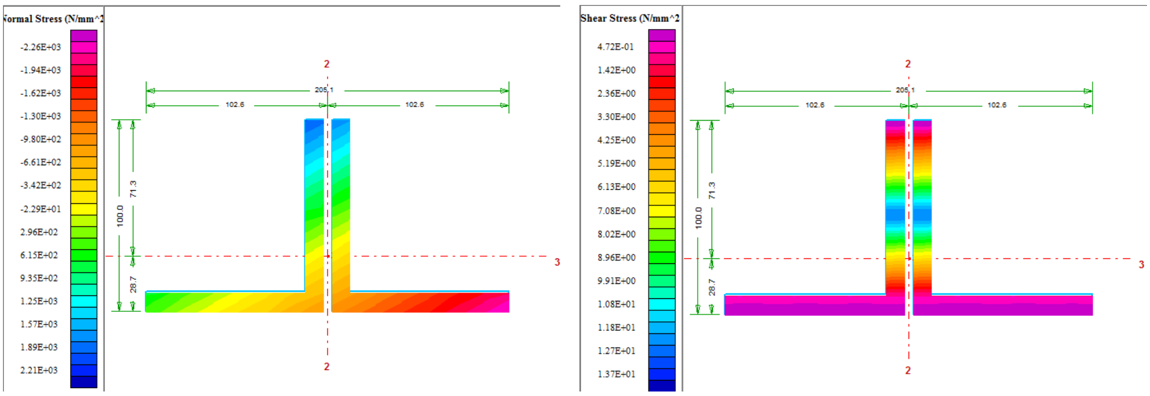

Fig. 10 Distribution of normal (left) and shear (right) stresses in 2L100×100×10 mm (tee array)

mm and L80×80×8 mm) and also 2L80×80×8 mm in both box profile and tee array can meet the requirements of area, moment of inertia and stress distribution. Furthermore, they cannot withstand the exerted loads on pipe fore-poling system. Therefore, 2L100×100×10 mm in both box profile and tee array are to be constituted for pipe fore-poling system as the support of the adit tunnel.

Moreover, the comparison between box profile and tee array in 2L100×100×10 mm and 2L80×80×8 mm shows that the values of normal and shear stresses distributing in the section are lower in box profile so the strength increases in the 2L100×100×10 mm in box profile rather than

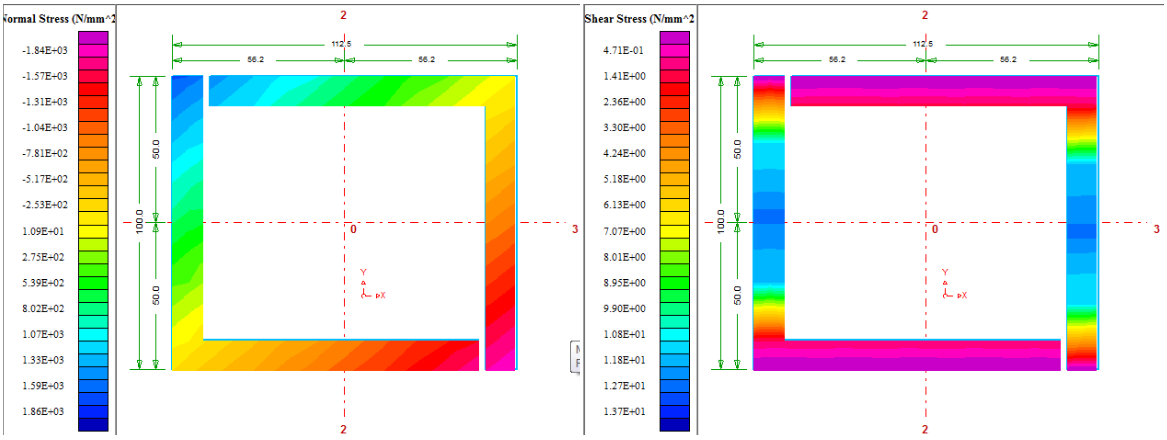

Fig. 11 Axial stress distribution in 2L100×100×10 mm (box profile)

Fig. 12 L-profile implementation in the adit tunnel

tee array. However, in the studied adit tunnel, 2L100×100×10 mm in tee array has been chosen because of its simpler installation.

Normal and shear stresses distributions under axial load and bending moment for 2L100×100×10 mm in tee array and box profile are indicated in Figs. 10 and 11, respectively.

Based on Fig. 10, the range of axial stress is between -2260 to 2210 N/mm^2 while the range of shear stress is between 0.472 to 13.7 N/mm^2 in tee array. Also, in box profile, as it is clear in Fig.11, the range of axial stress is between -1840 to 1860 N/mm^2 while the range of shear stress is between 0.471 to 13.7 N/mm^2.

Two image of the finished L-profile is given in Fig. 12.

4.3 Investigation of interaction diagrams of the sections

Axial force versus moment diagram of retaining capacity of different discussed sections is shown in Fig. 13. It can be seen that 2L100×100×10 mm in both box profile and tee array are more capable of sustaining loads rather than pipe fore-poling section so they are exchangeable.

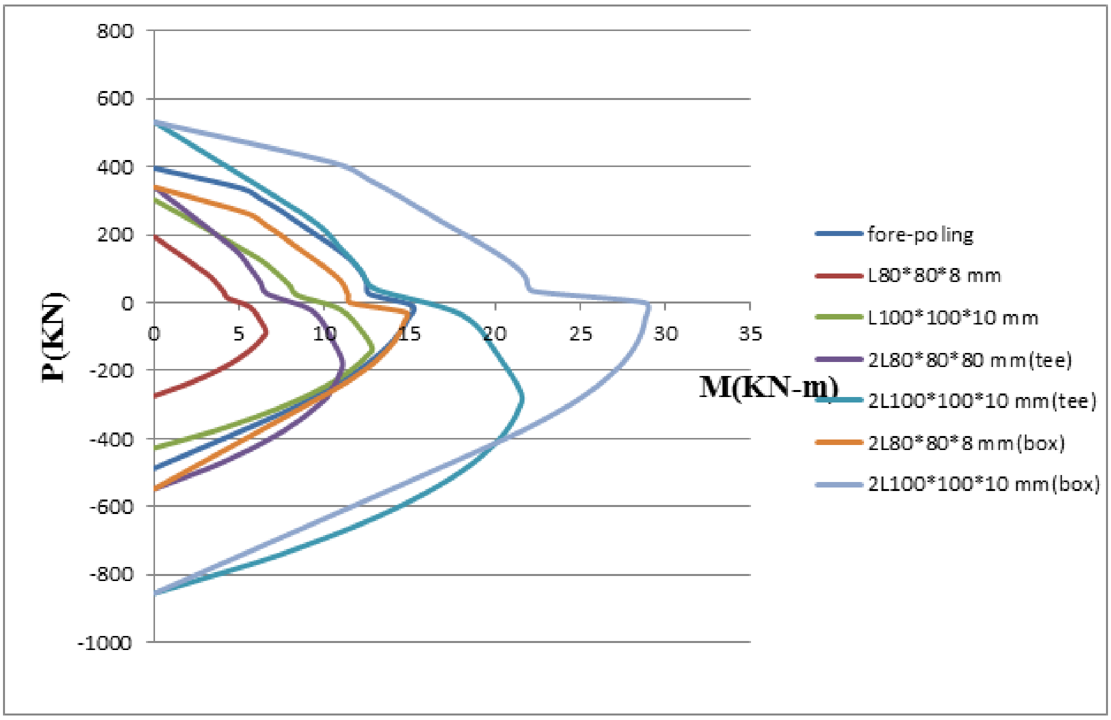

Fig. 13 Axial force-moment (P-M) interaction diagram for different sections

5. Results and validation

In order to monitor the tunnel behavior, a five-point convergence meter during construction of the tunnel is strongly suggested. The convergence pins in each tunnel section include one on the crown of the tunnel and four on the two side walls; these stations are repeated every 20 m along the tunnel. Installation and measurement are carried out simultaneously with the drilling and in the minimum distance from the working face in order to be able to record the minutest changes. Regarding the fact that construction of the adit tunnel utilizes the top and bench drilling method in which the top half is drilled where the deformations occur, three convergence pins were installed in this area, according to the timetable. In the next stage, when the lower section is being drilled, two other pins are installed in this area to control the total displacement.

Within the part of the tunnel in which the pre-support system of the umbrella arch is installed, there are two monitoring stations (tunnel sections) at 0+134 and 0+154 km. The convergence trend of these sections along with the reasons of the sharp changes in diagrams is given in Fig. 14. The results from reading the convergence of the spring lines (L1-R1) of the two stations show that horizontal convergence values for the two stations are 55 and 54 mm. Also, the horizontal displacement calculated from the numerical modeling for each end point of the arch (spring line) is equal to about 29 mm (Fig. 15). Therefore, the results from numerical modeling closely matched those from periodical readings of the instrumentation.

According to the diagram presented by Sakurai, underground openings will be stable if the occurring strain is smaller than the allowable strain, i.e., the occurring strain is below hazard warning level I. Furthermore, underground openings will encounter severe risk when the occurring

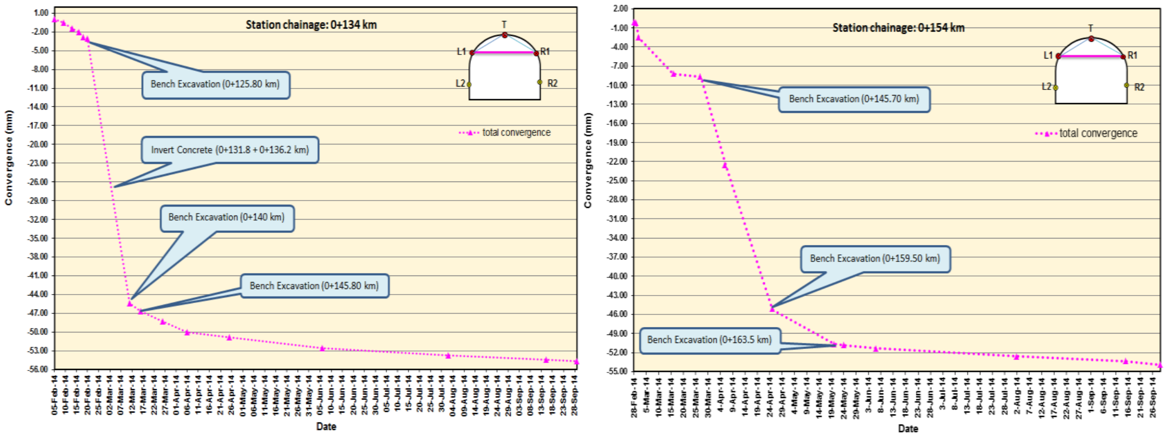

Fig. 14 Convergence of L1-R1 at 0+134 km (left) and at 0+154 km (right) stations

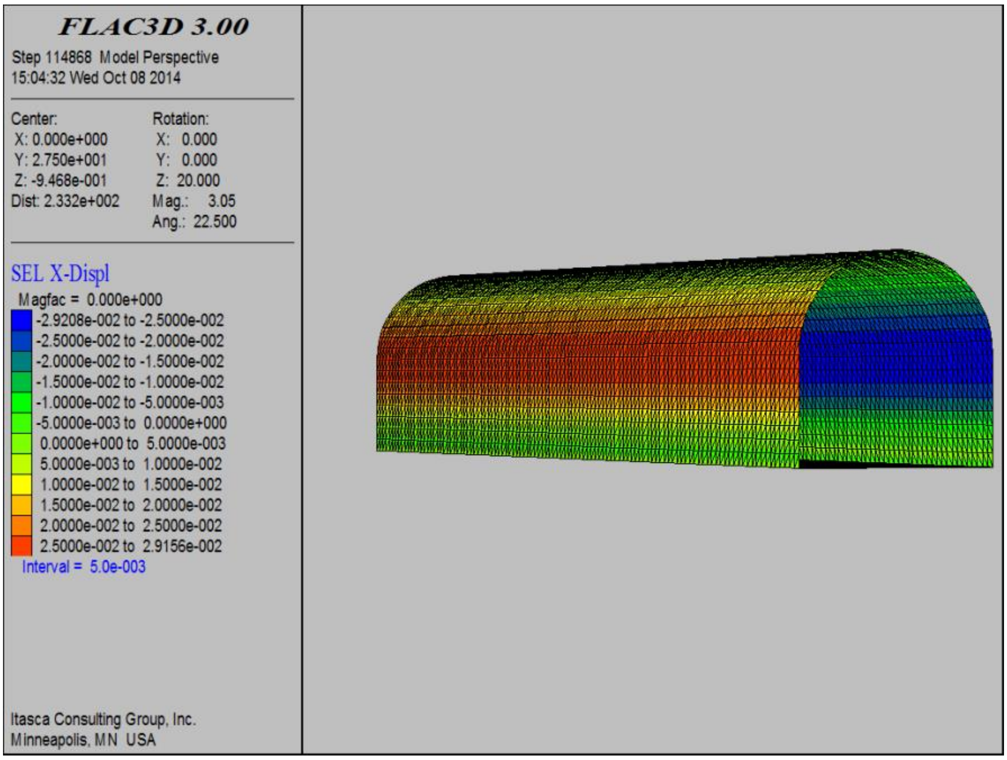

Fig. 15 Horizontal displacement around the tunnel with the Pre-support System

strain approaches the hazard warning level III (Sakurai *et al*. 1995).

It is recommended to consider the hazard warning level II as a base for tunnel designing while the hazard warning levels I and III represent the lower and upper limits of tunnel stability, respectively. It should be noted that these limits are based on allowable strain. Allowable displacement can be determined using Eq. (1) and the value of critical strain. Eq. (1) can be expressed as follows

Table 13 The values of allowable displacements and critical strain in different hazard warning levels of Sakurai

Allowable displacement (cm)			Critical strain (%)			Soil type
Warning level III	Warning level II	Warning level I	Warning level III	Warning level II	Warning level I	
14.157	6.039	2.576	0.038	0.016	0.007	SC
17.940	7.653	3.265	0.048	0.020	0.009	CL

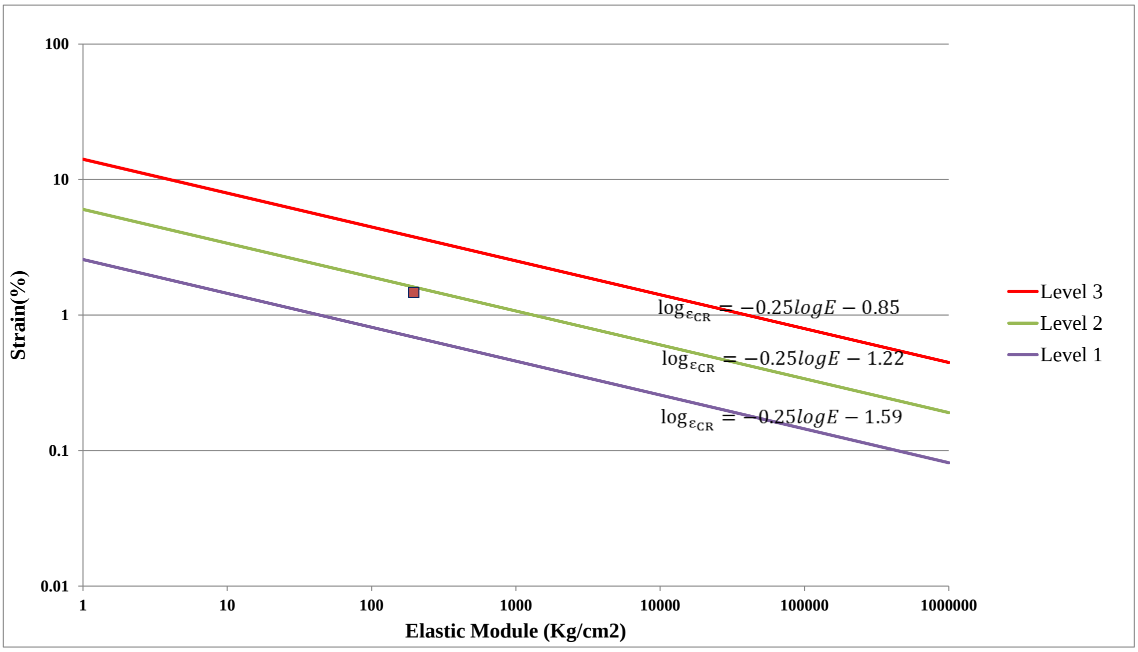

Fig. 16 Stability analysis of the adit tunnel by different hazard warning levels of Sakurai

$$\varepsilon_c = \frac{u_c}{a} \tag{1}$$

Where a is tunnel radius and u_c is allowable displacement.

After the evidences, the results of different experiments carried out in the site and the tunnel route materials were studied carefully by considering all the contributing factors, they led us to calculate the amounts of allowable displacements related to various hazard warning levels of Sakurai. The results of these calculations are presented in Table 13. Additionally, a comparison has been made between these results and the monitoring ones. All such considerations help us to assess the tunnel stability as accurate as possible.

According to Sakurai's criteria as it is shown in Fig. 16, the amount of tunnel displacement is just below the hazard warning level II but it can be claimed that static stability of the support system is ensured because the dips of convergence diagrams are approaching the horizontal line. Based on Fig. 17, investigation of the interaction diagram of the support system verifies this claim.

At Axial force-moment (P-M) interaction diagram study, since the tunnel lining is meant for permanent support, the primary support system including lattice girder and shotcrete with safety

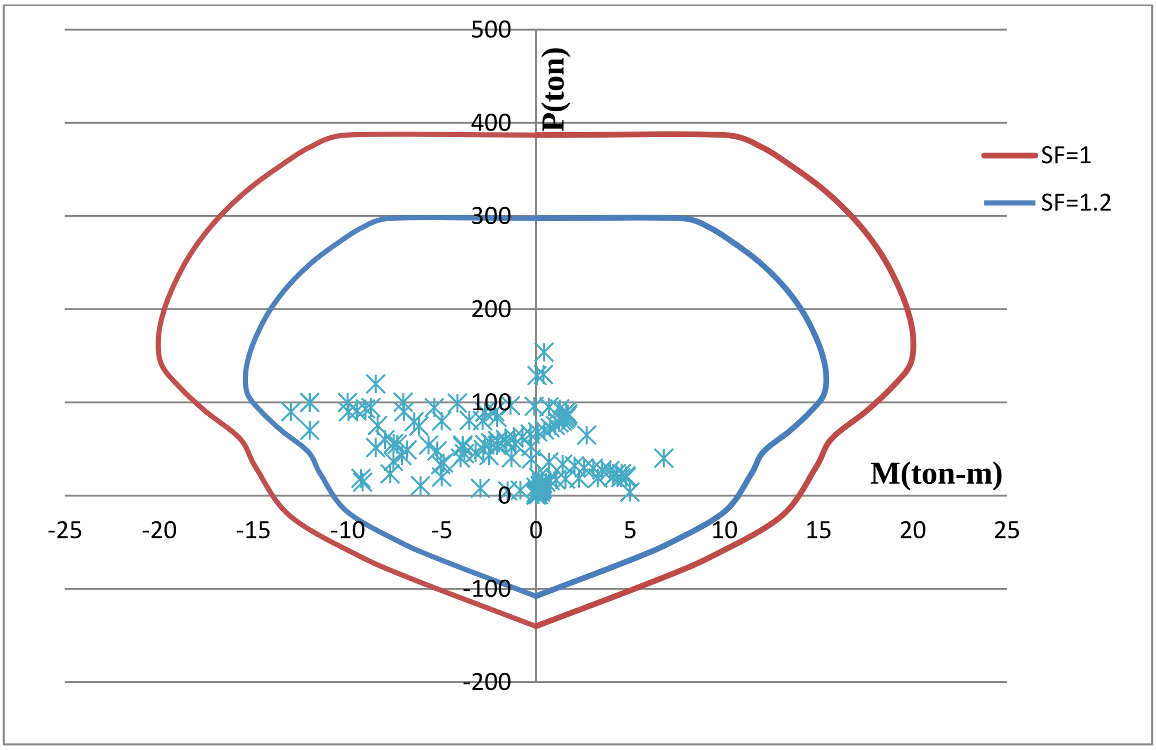

Fig. 17 Axial force-moment (P-M) interaction diagram for primary support system

factor of 1.2 was designed. The interaction curve for the primary support system, when pre-support system is being performed in different tunnel sections, is shown in Fig. 17. As it is clear, all measures are within the acceptable limits of axial force and bending moment. Also it should be noted that the diagrams are for excavation both the top and bench part, and in all cases the force and moment values are within an envelope with safety factor of 1.2.

6. Conclusions

According to the obtained results, it can be concluded that:

• Based on the modeling and studying the plastic zone and the displacements around the tunnel, the use of pipe fore-poling system and L-profiles leads to a significant decrease in the plastic zone as well as in the displacements around the tunnel. Therefore the tunnel will be more stable.

• The distribution of the forces and the displacement in the central pipe on the crown of the tunnel is different from those in pipes around the tunnel. In the top pipe, the vertical force is the maximum. In vertical loading of the pipes in the top half of the tunnel's arch, the maximum force occurs at the first one-third of the pipe, whereas, in the pipes in the lower half of the arch, the maximum force occurs in the first quarter of the pipe. In fact, the location of the maximum force will change with the change in the location of tunnel arc.

• Due to the decrease in the cantilever effects of grout at the end of the pipe and the decrease in the length of the pipe in the disturbed zone in front of the working face it is necessary to provide the second series of the pipes with appropriate overlap. The minimum length of overlap is equal to the length of the disturbed zone in front of the working face. With regard to the disturbed area of the adit tunnel face and the results of the modeling the optimum length of overlap is 2.5 m.

• The alternative section for steel pipes filled with cement grout can be a 2L100×100×10 mm in box profile or tee array.

• Neither of L80×80×8 mm nor 2L80×80×8 mm can be replaced with the mentioned pipe fore-poling system.

• In double equal angle sections, the values of normal and shear stresses distributed in the sections are less in box profile rather than tee array. Therefore, the 2L100×100×10 mm in box profile is recommended as an alternative section for pipe fore-poling system.

References

Aksoy, C.O. and Onargan, T. (2010), "The role of umbrella arch and face bolt as deformationpreventing support system in preventing building damages", *Tunnel. Underg. Space Tech.*, **25**(5), 553-559.

Barisone, G., Pigorini, B. and Pelizza, S. (1982), "Umbrella arch method for tunnelling in difficult conditions-analysis of Italian cases", *Proceedings of the Fourth Congress International Association of Engineering Geology*, New Delhi, **4**, 15-27.

Carrieri, G., Fiorotto, R., Grasso, P. and Pelizza, S. (2002), "Twenty years of experience in the use of the umbrella-arch method of support for tunnelling", *4th International Workshop on Micropiles*, Venice, Italy.

Carrieri, G., Grasso, P.G., Mahtab, A. and Pelizza, S. (1991), "Ten years of experience in the use of umbrella-arch for tunnelling", *Proceedings of the Congress on Soil and Rock Improvement in Underground Works*, Milano, **1**, 99-111.

Elyasi, A., Javadi, M., Moradi, T., Moharrami, J., Parnian, S. and Amrac, M. (2016), "Numerical modeling of an umbrella arch as a pre-support system in difficult geological conditions: a case study", *Bul. Eng. Geology Environ.*, **75**, 211-221.

Gangale, G., Corona, G. and Pelizza, S. (1992), "The Messina-Palermo motorway: complex rock masses and tunnelling problems", *Tow. New World. Tunnel.*, **2**, 873-880.

Haruyama, K., Teramoto, S., Harada, H. and Mori, M. (2001), "Construction of urban expressway tunnel with special large cross-section by NATM Metropolitan Inter-city Highway (ken-O-Do) Ome Tunnel", *International Symposium, Modern Tunnelling Science and Technology*.

Hoek, E. (2004), "Numerical modeling for shallow tunneling in weak rock", Discussion Paper # 3.

Kamata, H. and Mashimo, H. (2003), "Centrifuge model test of tunnel face reinforcement by bolting", *Tunnel. Underg. Space Tech.*, **18**(2-3), 205-212.

Kim, S.H., Baek, S.H. and Moon, H.K. (2005), "A study on the reinforcement effect of umbrella arch method and prediction of tunnel crown and surface settlement", Ed. Solak, E., Underground Space Use, Analysis of the Past and Lessons for the Future.

Fethi, K. (2015), "3D numerical study of tunnel advance core reinforcement: application on tunnel T4 from the algerian east-west highway", *Jordan J. Civil Eng.*, **9**(2), 139-149.

Lunardi, P. (2000), "The design and construction of tunnels using the approach based on the analysis of controlled deformation in rocks and soils", *Tunnels and Tunnelling International- Supplement*, May.

Mair, R.J. (2008), "Tunneling and geotechnics: new horizons", *Geotechnique*, **58**(9), 695-739.

Murata, M., Okazawa, T., Harunaka, K. and Tamai, A. (1996), "Shallow twin tunnel for six lanes beneath densely residential area", *North Am. Tunnel.*, **96**, 371-380.

Ocak, I. (2008), "Control of surface settlements with umbrella arch method in second stage excavations of Istanbul Metro", *Tunnel. Underg. Space Tech.*, **23**(6), 674-681.

Sakurai, S., Kawashima, I. and Otani, T. (1995), “A criterion for assessing the stability of tunnels”, *ISRM International Symposium*, **2**, 969-973.

Sekimoto, H., Kameoka, Y. and Takehara, H. (2001), “Countermeasures for surface settlement in constructing shallow overburden urban tunnels penetrated through active fault”, *International symposium, Modern Tunneling Science and Technology*, 711-716.

Shin, H.S., Han, K.C., Sunwoo, C., Choi, S.O. and Choi, Y.K. (1999), “Collapse of a tunnel in weak rock and the optimal design of the support system”, *Proceedings of the Ninth International Congress on Rock Mechanics*, Paris, France.

Shin, J.H., Choi, Y.K., Kwon, O.Y. and Lee, S.D. (2008), “Model testing for pipe-reinforced tunnel heading in a granular soil”, *Tunnel. Underg. Space Tech.*, **23**(3), 241-250.

Singh, B. and Goel, R.K. (2006), *Tunnelling in Weak Rocks*, Elsevier Geo-Engineering Book Series, Vol. 5. Elsevier Ltd, Oxford.

Federal Highway Administration (FHWA) (2009), “Technical Manual for Design and Construction of Road Tunnels Civil Elements”.

Volkmann, G.M. and Schubert, W. (2007), “Geotechnical model for pipe roof supports in tunneling”, *Proceeding of the 33rd ITA-AITES World tunneling congress, underground spaced the 4th dimension of metropolises*, Taylor & Francis Group, London.

Yoo, C. and Shin, H.K. (2003), “Deformation behaviour of tunnel face reinforced with longitudinal pipes-laboratory and numerical investigation”, *Tunnel. Underg. Space Tech.*, **18**, 303-319.

CC